SIMULATION AND EXPERIMENTAL CHARACTERIZATION OF A 2-D, 3-MHZ CAPACITIVE MICROMACHINED ULTRASONIC TRANSDUCER (CMUT) ARRAY ELEMENT

Ö. Oralkan, X. C. Jin, F. L. Degertekin, and B. T. Khuri-Yakub

Edward L. Ginzton Laboratory
Stanford University
Stanford, CA 94305-4085

Abstract— **In this paper, a 400-μm × 400-μm, 2-D capacitive micromachined ultrasonic transducer array element is experimentally characterized, and the results are found to be in agreement with theoretical predictions. As a receiver the transducer has a 1.8 × 10^{-7} nm/$\sqrt{Hz}$ displacement sensitivity, and, as a transmitter, it produces 16.4 kPa/V of output pressure at the transducer surface at 3 MHz. The transducer also has more than 100% fractional bandwidth around 3 MHz, which makes it suitable for ultrasound imaging. The radiation pattern measurements indicate a 3-dB acceptance angle of ± 35 degrees in agreement with the theoretical predictions.**

Keywords— **Ultrasonic transducer, 2-D array, capacitive micromachined transducer**

I. Introduction

Two-dimensional ultrasonic phased arrays have great importance for the realization of high frame-rate, real-time, 3-D ultrasound imaging systems. However, there are some major obstacles that limit the development of such imaging systems. A large number of array elements necessitates hundreds of active transducer channels, and there are severe difficulties in fabricating the arrays and providing individual electrical connections [1]. Another performance-limiting factor is the small element size. In order to reduce grating lobes, the interelement spacing must be less than the wavelength in the propagating medium. The small size of the elements limits the transmit power and degrades the receive sensitivity, making it difficult to achieve a large total dynamic range.

The capacitive micromachined ultrasonic transducers overcome many of the drawbacks of piezoelectric transducers. Besides their performance attributes (bandwidth and sensitivity), cMUTs provide advantages in ease of fabrication, size reduction, low self-noise, and the potential for electronic integration. Fabrication of 1-D and 2-D arrays of cMUTs and interconnects are quite simple and straightforward as compared to piezoelectric transducer arrays [2]-[4]. The transducer arrays can be integrated with standard CMOS electronics using through-chip interconnects and a flip-chip bonding technology [5].

This paper presents the experimental characterization of a 2-D cMUT array element and comparisons with the theoretical results. Further improvements in the performance of the cMUT are predicted after the validity of the cMUT equivalent circuit model is confirmed.

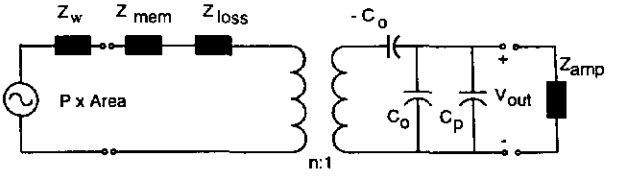

Fig. 1. Electrical equivalent circuit of the cMUT.

II. Transducer Electrical Equivalent Circuit Model

A cMUT cell consists of a metalized membrane (top electrode) suspended above a heavily doped silicon substrate (bottom electrode). There are many cells in a transducer element, and the elements are used to make 1-D or 2-D arrays. The operation of the cMUT can be explained as follows. A DC voltage is placed between the metalized membrane and the substrate. The membrane is attracted toward the bulk, and stress within the membrane resists the attraction. Ultrasound is generated by driving the membrane with an alternating voltage. If the biased membrane is subjected to ultrasound, detection currents are generated.

The receiving cMUT detects small ultrasonic signals. Thus, small signal analysis can be used. The small signal equivalent circuit of a cMUT is a two-port network. We use the Mason equivalent circuit where the electrical domain (voltage and current) is represented at one port, and the mechanical domain (force and velocity) is represented at the other port, as shown in Fig. 1 [6]. The detailed derivation of the model parameters for the cMUT is given in a recent paper [7]. In this equivalent circuit, Z_w corresponds to the mechanical impedance of water. Z_{mem} is the mechanical impedance of the membrane, and Z_{loss} accounts for the total loss. The ideal transformer in the circuit transforms velocity, a mechanical quantity, into electrical current. C_p represents the parasitic capacitance.

III. Experimental Characterization of the cMUT

The physical parameters of the cMUT used in these experiments are listed in Table I. The active area of the cMUT is 46% of the total 400-μm × 400-μm element area.

In immersion applications the impedance of the mem-

0-7803-5722-1/99/$10.00

TABLE I

PHYSICAL PARAMETERS OF THE CMUT.

d	diameter	$36\mu m$
t_n	membrane thickness	$0.80\mu m$
t_a	air-gap thickness	$0.10\mu m$
t_b	insulating layer thickness	$0.15\mu m$
N	number of cells in the element	72

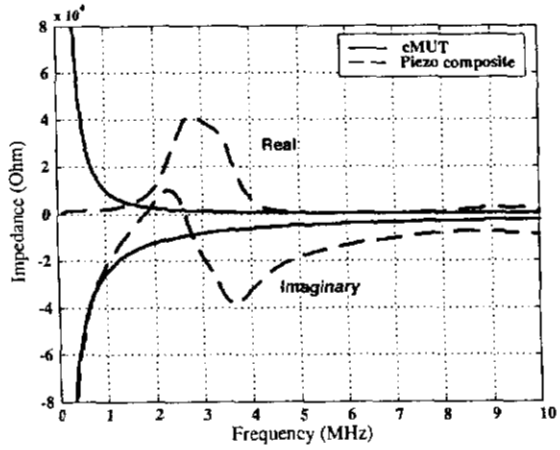

Fig. 2. Electrical input impedance of the cMUT and the piezocomposite transducer.

brane is smaller than the impedance of water and can be ignored in comparison. Thus, the input impedance of an immersion transducer has no resonance and consists of an RC circuit. The bandwidth and the efficiency of the transducer are determined by the termination at the electrical port. The wideband characteristic of the cMUT impedance is compared with the resonant behavior of the impedance of a piezocomposite transducer in Fig. 2. The DC bias voltage on the cMUT is set at 105 V. The value of the parasitic capacitance in the equivalent circuit model is determined according to the measured electrical input impedance of the cMUT. The parasitic factor, which is the ratio of the parasitic capacitance (C_p) to the device capacitance (C_0) is found to be eight in simulations for the measured device. This device has a C_0 of 0.715 pF. In order to characterize the cMUT in receive mode, the experimental setup shown in Fig. 3 is used. In this experiment a piezoelectric transducer (Panametrics V109) is used as the transmitter. The pressure output of the piezoelectric transmitter is characterized using a calibrated hydrophone at a distance of 7.5 cm. The cMUT is placed at the same location, and the DC bias voltage is set at 105 V. The received signal is amplified by a preamplifier designed for minimum insertion loss. The amplifier has a 32 dB midband gain and a 3-dB bandwidth of 3.5 MHz centered at 2.5 MHz.

The measured impulse and frequency responses are shown in Fig.4. This frequency response is limited by the transmitter and amplifier responses, and not the transducer's own response. We note in Fig. 4 that there is an

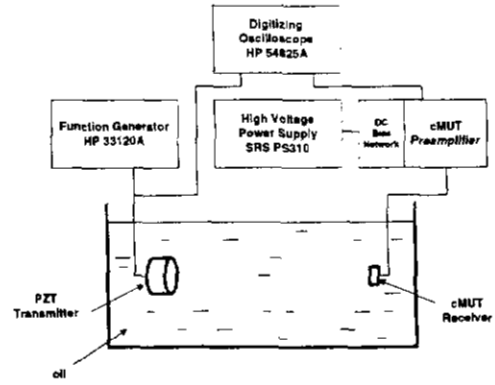

Fig. 3. Experimental setup used for cMUT receive mode characterization.

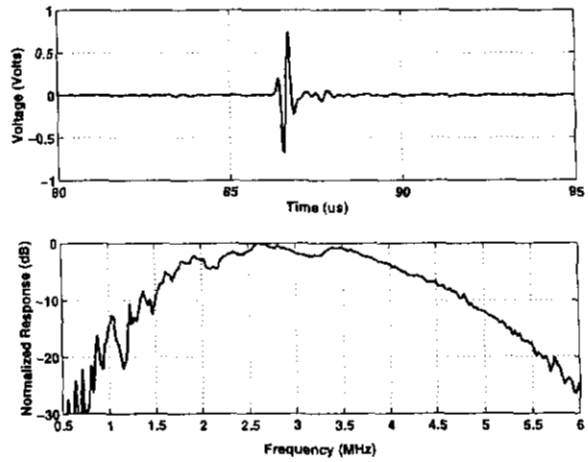

Fig. 4. Impulse and frequency responses of the 2-D cMUT array element.

abrupt change at around 1-1.5 MHz in the cMUT response. This change is due to lateral coupling of acoustic energy to neighboring array elements. The frequency at which this lateral coupling occurs depends on the spatial periodicity of the array and the material properties of the fluid medium. This lateral coupling of acoustic energy in cMUT arrays is currently under research.

The measured output signal-to-noise ratio (SNR) and the results of the HSPICE simulation for the complete receiver system are shown in Fig. 5. The measured SNR is about 45 dB/Pa/Hz, in agreement with the simulations. The minimum detectable pressure for the system is 5 mPa/$\sqrt{Hz}$, corresponding to a 1.8×10^{-7} nm/$\sqrt{Hz}$ displacement at 3 MHz.

The amplifier used in these experiments is suboptimal; however it served well for characterization purposes. We simulated the system with another amplifier with an 8.2-MΩ input resistance, 0.25-pF input capacitance, 15 nV/$\sqrt{Hz}$ input-referred equivalent noise voltage, and negligible input-referred noise current. In this amplifier the insertion loss is not taken as a design constraint. The improvement in SNR with the use of this amplifier is shown by the solid line in Fig. 6. Another factor degrading the receive

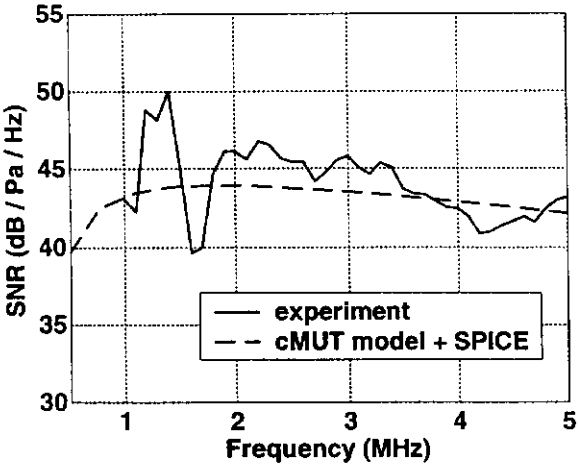

Fig. 5. Simulated and measured output SNR.

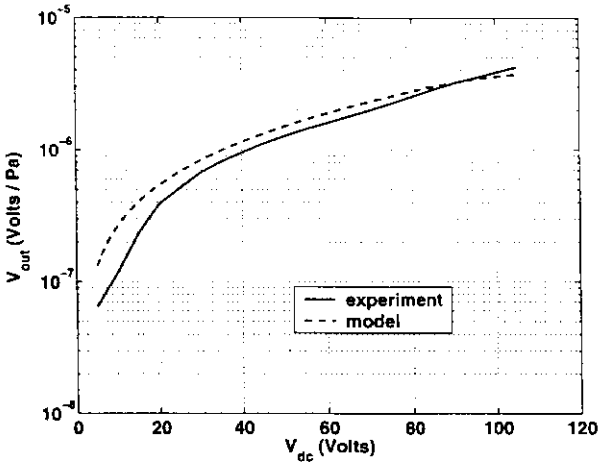

Fig. 7. DC bias sensitivity of the cMUT in receive mode.

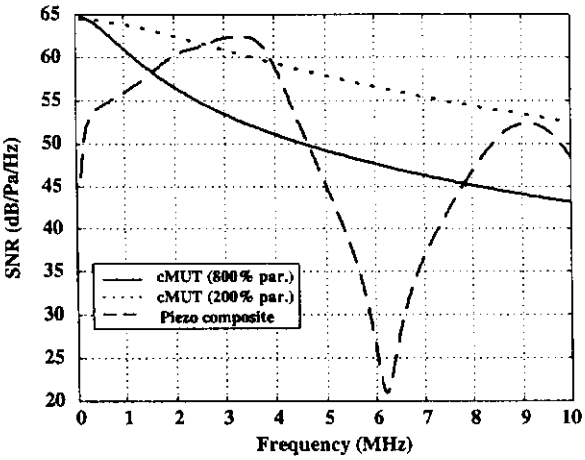

Fig. 6. Simulated SNR with the amplifier with a better noise performance.

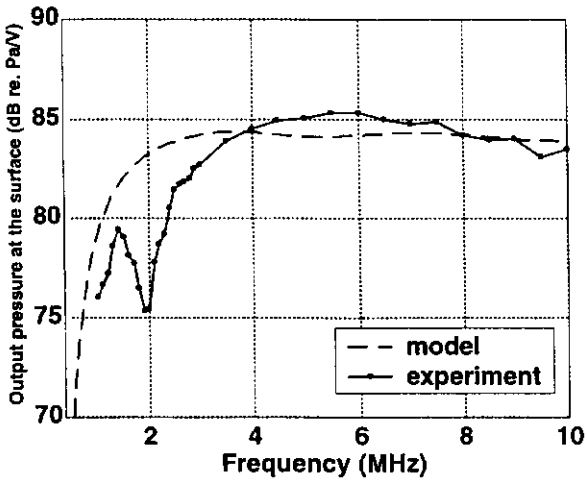

Fig. 8. Output pressure produced by the cMUT on its surface.

performance is the large parasitic capacitance. We expect a dramatic decrease in the parasitic capacitance with the use of the through-chip interconnect scheme [5]. The simulation result for the cMUT with 200% C_p is shown in Fig. 6 together with piezocomposite transducer simulation with the same amplifier for comparison.

The receive performance improves by the use of through-chip interconnect scheme, which decreases the parasitic capacitance. An optimized amplifier for the given transducer also increases the noise performance of the receiver system.

The dependence of the cMUT response on the DC bias voltage can also be predicted by the model as shown in Fig. 7.

In transmit experiments the DC bias voltage on the cMUT is again set at 105 V. The cMUT is driven by the function generator. The pressure produced by the cMUT is measured using the calibrated hydrophone in the far field. The pressure at the cMUT surface is calculated by taking the diffraction loss into account. The measured and simulated output pressure figures at the transducer surface are shown in Fig. 8. In simulations the medium is modeled as a load with complex impedance. The cMUT produces a 16.4 kPa/V output pressure on its surface at 3 MHz. We note that the pressure is plotted up to 10 MHz in Fig. 8 showing a broadband response.

As a measure of the total tolerable loss in pulse-echo operation, a dynamic range for the transducer can be defined as the ratio of the pressure output of the transducer to the minimum detectable pressure. The cMUT used in this work achieved a total dynamic range of 150 dB/Hz for 10 V input voltage at 3 MHz. The measured and simulated dynamic ranges are shown in Fig. 9 for 1 V input voltage. The simulation result using the alternative amplifier and 200% C_p shows that a 160 dB/Hz dynamic range for 10 V input voltage is achievable at 3 MHz.

The radiation pattern of the 2-D cMUT array element at 3 MHz is shown in Fig. 10. The measured beam profile is in excellent agreement with the theoretical prediction,

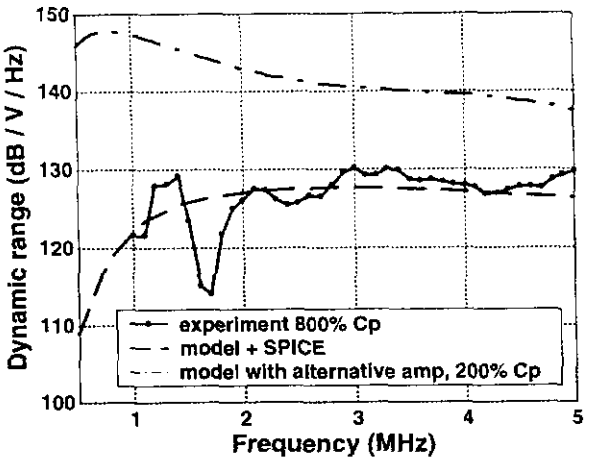

Fig. 9. Dynamic range of the transmit-receive system.

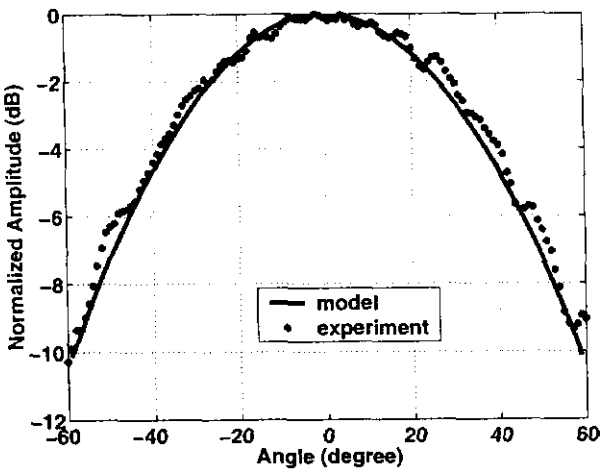

Fig. 10. Radiation pattern of the 2-D cMUT array element at 3 MHz.

which assumes a piston transducer with equal active area. The 3-dB acceptance angle is measured as ± 35 degrees. No significant cross coupling is observed. In a 2-D array, each element acts as a point source transmitter and receiver. Piston-like behavior of each cMUT array element with small acoustic and electrical cross coupling makes it suitable for imaging applications.

IV. Conclusion

In this paper a 2-D cMUT array element has been characterized in both receive and transmit modes. Experimental results are in good agreement with theoretical predictions. These results confirm the validity of the cMUT equivalent circuit model. The model can be used to predict further improvements in performance and, in fact, is a powerful tool for future device designs. Reduction in parasitic capacitance and optimizing the amplifier will increase the system performance for the current transducer design. The performance can be improved further by increasing the active area. In radiation pattern measurements, 2-D cMUT array element demonstrated a wide acceptance angle with no significant cross coupling. In this paper, we have demonstrated that the cMUT is an attractive alternative to piezoelectric transducers. The ease of fabrication and electronics integration, large bandwidth, and the large dynamic range of the cMUT make it a superior transducer choice for 2-D phased arrays.

Acknowledgments

This work was supported by the United States Office of Naval Research. The authors thank Mr. A. Dâna for his help in the Ginzton Machine Shop.

References

[1] D. H. Turnbull and F. S. Foster, "Fabrication and characterization of transducer elements in two-dimensional arrays for medical ultrasound imaging," *IEEE Trans. Ultrason., Ferroelec., Freq. Contr.*, vol. 39, pp. 464-474, Jul 1992.

[2] X. C. Jin, I. Ladabaum, and B. T. Khuri-Yakub, "The microfabrication of capacitive ultrasonic transducers," *IEEE/ASME J. Microelectromech. Syst.*, vol. 7, pp. 295-302, Sep 1998.

[3] X. C. Jin, F. L. Degertekin, S. Calmes, X. J. Zhang, I. Ladabaum, and B. T. Khuri-Yakub, "Micromachined capacitive transducer arrays for medical ultrasound imaging," in *Proc. IEEE Ultrason. Symp.*, Sendai, Japan, 1998, pp. 1877-1880.

[4] X. C. Jin, I. Ladabaum, F. L. Degertekin, S. Calmes, and B. T. Khuri-Yakub, "Fabrication and characterization of surface micromachined capacitive ultrasonic immersion transducers," *IEEE/ASME J. Microelectromech. Syst.*, vol. 8, pp. 100-114, Mar 1999.

[5] X. C. Jin, S. Calmes, C. H. Cheng, F. L. Degertekin, and B. T. Khuri-Yakub, "Micromachined capacitive ultrasonic immersion transducer array," in *Dig. Tech. Papers Transducers'99*, Sendai, Japan, 1999, pp. 1500-1503.

[6] W. P. Mason, *Electromechanical Transducers and Wave Filters*. New York: Van Nostrand, 1942.

[7] I. Ladabaum, X. C. Jin, H. T. Soh, A. Atalar, and B. T. Khuri-Yakub, "Surface micromachined capacitive ultrasonic transducers," *IEEE Trans. Ultrason., Ferroelect., Freq. Contr.*, vol. 45, pp. 678-689, May 1998.